Editors' Suggestion | Featured in Physics

Topological Defect Formation in a Phase Transition with Tunable Order

Fumika Suzuki[1,2,*] and Wojciech H. Zurek[1]
[1]Theoretical Division, Los Alamos National Laboratory, Los Alamos, New Mexico 87545, USA
[2]Center for Nonlinear Studies, Los Alamos National Laboratory, Los Alamos, New Mexico 87545, USA

(Received 18 December 2023; accepted 15 April 2024; published 11 June 2024)

The Kibble-Zurek mechanism (KZM) describes the nonequilibrium dynamics and topological defect formation in systems undergoing second-order phase transitions. KZM has found applications in fields such as cosmology and condensed matter physics. However, it is generally not suitable for describing first-order phase transitions. It has been demonstrated that transitions in systems like superconductors or charged superfluids, typically classified as second order, can exhibit weakly first-order characteristics when the influence of fluctuations is taken into account. Moreover, the order of the phase transition (i.e., the extent to which it becomes first rather than second order) can be tuned. We explore quench-induced formation of topological defects in such tunable phase transitions and propose that their density can be predicted by combining KZM with nucleation theory.

DOI: 10.1103/PhysRevLett.132.241601

The Kibble-Zurek mechanism (KZM) combines Kibble's observation of the inevitability of topological defect formation in cosmological phase transitions [1,2] with the theory proposed by one of us [3–5] that relates their density to the critical slowing down and, hence, to the universality class of the second-order phase transition. The resulting KZM predicts defect density as a function of the quench rate during second-order phase transitions, in both classical and quantum settings [6–27]. It finds applications in condensed matter physics [3–5], cosmological phase transitions [1,2,28–30], superconductors [31], liquid crystals [32,33], superfluids [34–36], ultracold chemistry [27], Bose-Einstein condensates [37–40], and quantum computing [41,42].

However, KZM is generally not suitable for describing first-order phase transitions. In [43], it has been demonstrated that the transitions associated with superconductors or superfluids can exhibit weakly first-order characteristics [44]. This should allow one to tune the order of the transition between the second and first order, with the weakly first-order characteristics in between. Given the critical properties shared between, e.g., smectic-A liquid crystals and superconductors, the transitions in liquid crystals can also exhibit a weakly first-order nature. In particular, there is now compelling evidence that the order of the Fredericks phase transition can be "tuned" in this manner [45].

In this Letter, we demonstrate that the formation of topological defects in those systems can resemble either a second-order or a first-order phase transition, or fall in between these two regimes (i.e., become weakly first-order). This variation depends on factors such as the strength of the first-order component in the free energy, the quench timescale, and the temperature.

While KZM has been investigated numerically [46–49] and experimentally [31–36,41,42,50–53], its applicability to weakly first-order or tunable phase transitions is an open question. The following analysis demonstrates that KZM can remain viable for predicting the density of defects generated in a phase transition with tunable order when it is integrated with thermally activated nucleation [54–58].

We note that Kibble suggested initially [1] that thermal activation determines the density of defects even in the second-order nonequilibrium phase transitions [59]. In contrast to KZM, thermal activation would result in defect densities independent of the quench rate. Nevertheless, as we shall see, thermally activated nucleation can compete with KZM in determining the density of topological defects in the tunable transitions we consider.

Here, we first present numerical results illustrating the interplay of critical slowing down and thermally activated nucleation in the formation of topological defects in a phase transition with tunable order. We then provide an analytical interpretation of the results.

To explore KZM in a phase transition with tunable order, we examine the numerical evolution of a one-dimensional system governed by the equation of motion for a real scalar field ϕ. The equation is derived from the modified Landau-Ginzburg potential

$$V(\phi) = (\phi^4 - 2\epsilon\phi^2)/8 - c|\phi|^3/3, \tag{1}$$

where the first two terms account for the typical second-order phase transition behavior and the third term introduces the first-order characteristics as presented in [43] (see Fig. 1). Here, the constant c represents the strength of the term responsible for first-order nature of the phase transition.

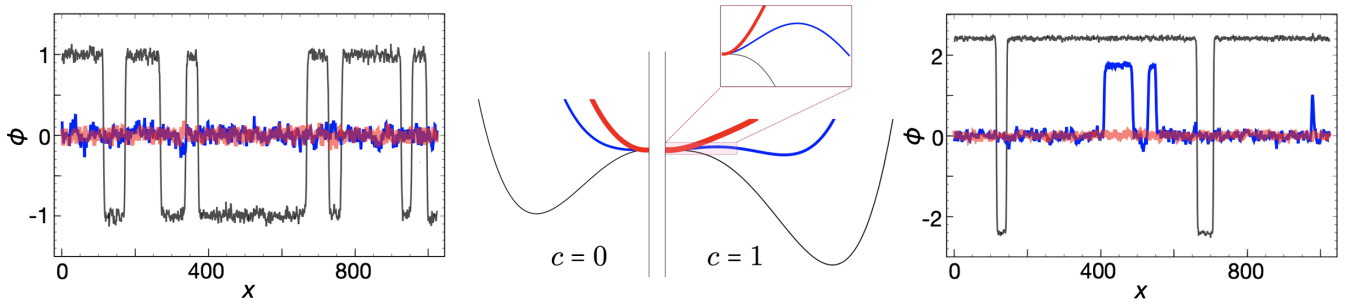

FIG. 1. Snapshots of ϕ and corresponding $V(\phi)$ following second-order phase transition with $c = 0$ (left) and phase transition with $c = 1$ (right). Plots of $\phi(x)$ at different stages of the quench, starting with $\epsilon = -1.5$ (thick red line), $\epsilon = -0.45$ (blue line), and $\epsilon = 1$ (thin black line) are shown.

We assume that ϵ follows a linear quench, $\epsilon(t) = t/\tau_Q$, with τ_Q representing the quench timescale.

The system is in contact with a thermal reservoir and it obeys the Langevin equation

$$\ddot{\phi} + \eta\dot{\phi} - \partial_{xx}\phi + \partial_\phi V(\phi) = \vartheta(x,t), \tag{2}$$

where the noise term ϑ has correlation properties

$$\langle \vartheta(x,t), \vartheta(x',t')\rangle = 2\eta\theta\delta(x'-x)\delta(t'-t) \tag{3}$$

with the temperature of the reservoir θ and η is the overall damping constant. In this Letter, we set $\eta = 1$.

When $c = 0$, we recover the ordinary second-order phase transition where ϵ measures the distance from the critical point. $t < 0$ and $t > 0$ represent the time before and after the transition at $\epsilon = 0$, respectively. This scenario was thoroughly investigated in [49].

When $c > 0$, a characteristic of a first-order phase transition emerges: for $\epsilon < -c^2$, the potential exhibits symmetry with a single minimum, similarly to a second-order phase transition. However, for $-c^2 < \epsilon < 0$, it develops two minima at $\phi = \pm(c + \sqrt{c^2+\epsilon})$ corresponding to the new phase in addition to the existing one at $\phi = 0$ representing the old phase, leading to nucleation associated with the first-order phase transition. The positions of these nucleation barrier peaks are $\pm\phi_{\text{barrier}}$, where $\phi_{\text{barrier}} = c - \sqrt{c^2+\epsilon}$, and their height is

$$h_{\text{barrier}} = -\frac{1}{24}\left(c - \sqrt{c^2+\epsilon}\right)^2\left[3\epsilon + 2c\left(c - \sqrt{c^2+\epsilon}\right)\right]. \tag{4}$$

This indicates that the positions ϕ_{barrier} and the height h_{barrier} of the nucleation barriers approach 0 as $\epsilon \to 0$. Hence, with both $c = 0$ and $c > 0$, the potential with two minima eventually emerges for $\epsilon > 0$. Figure 1 illustrates the snapshots of ϕ and corresponding $V(\phi)$ following second-order phase transition (left) and phase transition with nonzero c (right). For the second-order phase transition, ϕ initially fluctuates around its expectation value $\langle\phi\rangle = 0$ when $\epsilon < 0$. After the symmetry breaking takes place (i.e., $\epsilon > 0$), ϕ is forced to choose one of two minima and gradually settles locally around $\langle\phi\rangle \approx \pm\sqrt{\epsilon}$ while forming defects. For a phase transition with $c > 0$, ϕ follows a similar transition, except that nucleations can occur when $-c^2 < \epsilon < 0$. Our primary interest lies in assessing the impact of these nucleation events on the density of defects after the transition ($\epsilon > 0$).

Following the method described in [49], we numerically investigate the number of defects generated by phase transitions as a function of the quench timescale τ_Q. We initiate the time evolution obeying Eq. (2) with $\epsilon = -2$ and conclude it when ϵ reaches 5. The number of defects is determined by counting the points where $\phi = 0$ at $\epsilon = 5$. We performed 15 numerical simulations of the phase transition for each τ_Q and obtained Fig. 2. Black squares and dark red circles represent numerical results for $c = 0$ (purely second-order phase transition) and $c > 0$, respectively. The dashed black line represents the best fit of the black squares. The best fit corresponds to $n_{\text{KZM}} \propto \tau_Q^{-a}$, where $a = 0.267 \pm 0.029$, which agrees closely with the theoretical prediction of KZM, $a = 1/4$ [3–5]. As the quench timescale τ_Q increases, we notice a pronounced deviation of the dark red circles from the prediction of KZM depicted by the dashed black line. This departure can be attributed to the increased likelihood of nucleation events. In the middle panel, we have a decrease in the nucleation rate due to a low temperature $\theta = 0.001$. Because of the low nucleation rate, there is only a small overall deviation from the predictions of KZM. On the other hand, the right panel presents the results for larger value of $c = 2$, indicating a stronger first-order phase transition term in the potential (1). In this case, a significant departure from KZM is observed even when τ_Q is relatively small.

These plots can be understood as follows. When ϕ fluctuates around its expectation value $\langle\phi\rangle = 0$ initially, it starts to interact with the nucleation barriers at $t = t_1$ when $\sqrt{\langle\phi^2\rangle}$ is approximately equal to the location of the barriers ϕ_{barrier}. In the vicinity of $\phi = 0$, the potential can be approximated by a harmonic potential $V_{\text{har}}(\phi) = \frac{1}{2}\omega^2\phi^2$

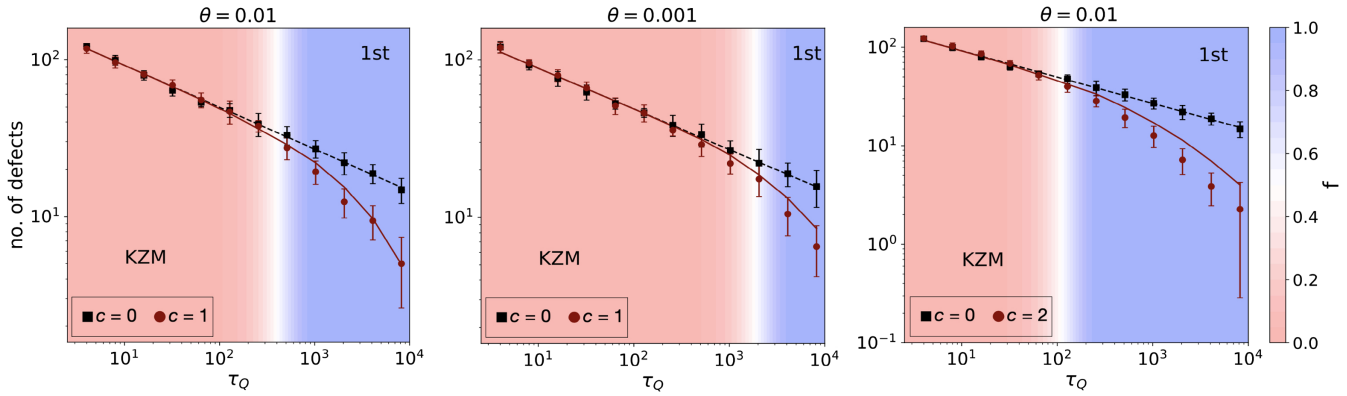

FIG. 2. Number of defects as a function of quench timescale τ_Q. Black squares represent numerical results for $c = 0$ where KZM is expected to hold. The dashed black line represents the best fit of the black squares. Dark red circles represent numerical results for $c = 1$, $\theta = 0.01$ (left), for $c = 1$, $\theta = 0.001$ (middle), and for $c = 2$, $\theta = 0.01$ (right), respectively. The solid dark red lines represent the number of defects derived from Eq. (10). The fraction of space $\mathfrak{f}$ occupied by the new phase due to nucleation events (7) is depicted using a color plot.

where ω is given by $V_{\rm har}(\phi_{\rm barrier}) = h_{\rm barrier}$. Since the temperature θ corresponds to the energy of ϕ, we have $\langle\phi^2\rangle \approx \theta/\omega^2$. Therefore, ϕ starts to interact with the barrier at t_1 when $(\theta/\omega^2)^{1/2} = \phi_{\rm barrier}$. After t_1, there is a possibility of nucleation occurring.

The nucleation rate per unit length of the metastable state around $\phi = 0$ is given by [54]

$$\Gamma[\epsilon(t)] = A\exp\{-B[\epsilon(t)]/\theta\}, \tag{5}$$

where

$$B[\epsilon(t)] = 2\int_0^{\phi_{\rm TP}} d\phi\sqrt{2V(\phi)}. \tag{6}$$

Here, $\phi_{\rm TP}$ is the classical turning point such that $V(\phi = 0) = V(\phi_{\rm TP}) = 0$. The prefactor A exhibits only a soft dependence on temperature and ϵ. In this Letter, we set $A \approx 0.4$ obtained numerically. Since ϵ is time-dependent, B and Γ are time-dependent. In particular, $B \to 0$ as $\epsilon \to 0$. This suggests that as the parameter ϵ approaches 0, the influence of the barriers becomes insignificant in comparison to the kinetic energy of the field $\langle\dot{\phi}^2\rangle$, given by the temperature θ. Then ϕ undergoes a transition to one of the two broken symmetry minima, much like what occurs in a second-order phase transition. In our model, this behavior is observed after time t_2 when the energy of the nucleation barriers becomes equal to the kinetic energy of ϕ, $B[\epsilon(t_2)] = \theta$ (Supplemental Material [60]).

The fraction of space $\mathfrak{f}$ occupied by the new phase due to nucleation events during the period between t_1 and t_2 can be obtained using the Avrami equation [61–65]. This equation describes the progress of phase transformations via a nucleation-growth process in first-order phase transitions, under the assumption that the transformation follows a sigmoidal function. It is applied in various areas, including cosmology, to describe the fraction of space that has undergone transition from the false vacuum to the true vacuum [66–68]. It can be derived by assessing the probability that a particular point in space is not enclosed within any true vacuum bubbles. In Supplemental Material [60], we provide a brief derivation of the equation by following [67,68]. The equation reads

$$\mathfrak{f} = 1 - \exp(-\Omega), \tag{7}$$

where

$$\Omega = \int_{t_1}^{t_2} \Gamma[\epsilon(t)]\mathcal{V}(t, t_2)dt. \tag{8}$$

Here, $\mathcal{V}(t, t_2) = \int_t^{t_2} v(\epsilon(\tau))d\tau$ represents the volume of a nucleated bubble at the time t_2, which was formed at time t. v is the bubble wall velocity. $\mathfrak{f}$ describes the fraction of space transformed to the new phase between t_1 and t_2, and $\mathfrak{f} = 1$ when the entire space is covered by the new phase through a nucleation-growth process during the time interval. The velocity v is dependent on θ, η, and ϵ. Since we fix θ and η during the time evolution in our model, we only analyze the ϵ dependence of v by numerical simulations as follows.

When ϵ with $-c^2 < \epsilon < 0$ is held fixed and time-independent, both the nucleation rate Γ and the velocity v become time-independent, and only a nucleation-growth process takes place. Then we have the general Avrami equation in one dimension written as

$$\mathfrak{f}_{\rm fixed} = 1 - \exp\left(-\frac{1}{2}v(\epsilon_{\rm fixed})\Gamma(\epsilon_{\rm fixed})t^2\right). \tag{9}$$

By fitting this equation to the numerical results of the time evolution of the fraction of space occupied by the new

phase at each fixed ϵ, we obtain the ϵ dependence of v, which will then be substituted into Eqs. (7), (8) in the following discussion (Supplemental Material [60]). For $c = 1$ and the temperature $\theta = 0.01$, $v(\epsilon) = 0.026\epsilon + 0.016$ was obtained by the method described above. For different values of c and θ, we repeated the same procedure to obtain corresponding v.

In the absence of nucleation events, the fraction of space occupied by the new phase due to nucleations is zero, i.e., $\mathfrak{f} = 0$. The field ϕ then would follow second-order phase transition behavior obeying KZM even in the presence of a nonzero c. Conversely, with an increase in $\mathfrak{f}$, the behavior of the first-order phase transition becomes dominant. It can be assumed that the density of defects for the fraction of space $\mathfrak{f}$ follows nucleation theory, while the density for the remaining space $(1 - \mathfrak{f})$ obeys KZM. The number of defects generated in a phase transition with tunable order can then be estimated as

$$n = \mathfrak{f} n_{\mathrm{nuc}} + (1 - \mathfrak{f}) n_{\mathrm{KZM}}, \tag{10}$$

where n_{KZM} obeys KZM in the second-order phase transition, i.e., $n_{\mathrm{KZM}} \propto \tau_Q^{-a}$ with $a = 1/4$ in our model. In general, the number of defects n_{nuc} generated by a nucleation-growth process increases with the increase in the nucleation rate Γ and decreases with the rise of the bubble wall velocity v. It is because a larger value of Γ leads to the growth of the number density of bubbles. Consequently, the distance between bubbles shortens, and the average time before a collision between two domains decreases. Conversely, the domain size increases for larger v, as bubbles grow more rapidly before the collision [58]. Since Γ is a complex function of ϵ, we numerically obtain the ϵ dependence of n_{nuc} by performing the nucleation process for each fixed ϵ. n_{nuc} exhibits an almost linear dependence on ϵ within the relevant small ϵ range of interest (i.e., $-c^2 < \epsilon < 0$). Numerically, we obtained the equation $n_{\mathrm{nuc}} \approx 144\epsilon + 74$ for $c = 1$ and $\theta = 0.01$ (Supplemental Material [60]). For different values of c and θ, we repeated the same procedure to derive the equation for n_{nuc}. Since ϵ changes over time during the phase transition, n_{nuc} also depends on time. We assume that the number of defects created by the nucleation-growth process throughout time evolution can be approximated by the time-averaged value, $n_{\mathrm{nuc}} \sim n_{\mathrm{nuc}}(\epsilon^*)$, where ϵ^* represents the value of ϵ at the time when the fraction of space occupied by the new phase reaches half of $\mathfrak{f}$, i.e., $\epsilon^* = \epsilon(t^*)$, where $\mathfrak{f}^* = 1 - \exp\left(-\int_{t_1}^{t^*} \Gamma[\epsilon(t)]\mathcal{V}(t, t^*)dt\right)$ and $\mathfrak{f}^* = \mathfrak{f}/2$ (Supplemental Material [60]). After t_2, the nucleation barriers diminish in comparison to the kinetic energy of ϕ, leading to a behavior similar to a second-order transition. The number of defects generated within this regime obeys KZM and is given by n_{KZM}.

The solid dark red lines in Fig. 2 correspond to the number of defects derived from Eq. (10). They show reasonable agreement with the numerical results represented by the dark red circles. The fraction of space $\mathfrak{f}$ occupied by the new phase due to nucleation events (7) is depicted using a color plot. The phase transition occurs so rapidly that ϕ does not have sufficient time to interact with the nucleation barriers for the small quench timescale τ_Q. Consequently, nucleation does not occur, and the prediction of KZM remains valid in this regime. As τ_Q increases, $\mathfrak{f}$ also grows, and we see the transition into a regime where the behavior of the first-order phase transition becomes dominant, leading to a significant departure from KZM. As the temperature θ decreases, the nucleation rate also decreases, which in turn supports the applicability of KZM for even larger values of τ_Q. Conversely, with larger values of c, the nucleation barriers persist for a longer duration, resulting in deviations from the predictions of KZM even with relatively small τ_Q.

By modifying Eq. (10), we can estimate the discrepancy δ between the value predicted by KZM and the value obtained in a numerical simulation of a phase transition with tunable order,

$$\delta = \left| \frac{n - n_{\mathrm{KZM}}}{n_{\mathrm{KZM}}} \right| = \mathfrak{f} \left| 1 - \frac{n_{\mathrm{nuc}}}{n_{\mathrm{KZM}}} \right|. \tag{11}$$

Figure 3 shows the discrepancy as the function of c and temperature θ where the quench timescale $\tau_Q = 2048$. The left panel shows the discrepancy between the numerical results and the predictions of KZM. As c and θ increase, we observe a larger discrepancy, represented by the red color. For higher temperature θ, the kinetic energy of ϕ increases, thereby enhancing the likelihood of nucleation occurring prior to the second-order phase transition. For larger c, the nucleation barriers persist longer, thus increasing the occurrence of nucleation events. The fraction of space occupied by the new phase that forms due to nucleation events and the discrepancy can be evaluated using Eq. (7)

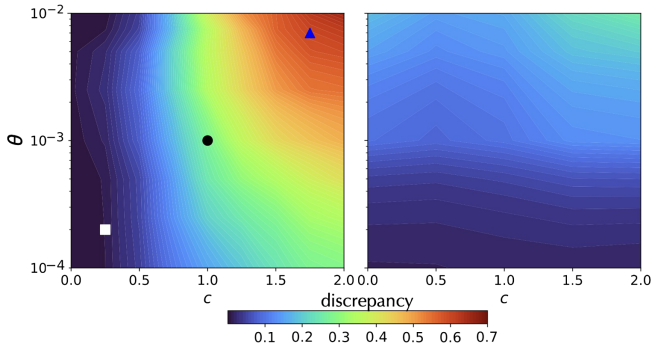

FIG. 3. The discrepancy between theory and numerical experiment as the function of c and temperature θ. The quench timescale $\tau_Q = 2048$. Left: the remaining discrepancy between the numerical results and the predictions of KZM alone. Right: the remaining discrepancy between the numerical results and the predictions of Eq. (10) that combines KZM and nucleation.

and Eq. (11). This yields $\mathfrak{f} = 0$, $\delta = 0$ for $c = 0.25$, $\theta = 0.0002$ (white square), $\mathfrak{f} = 0.55$, $\delta = 0.16$ for $c = 1$, $\theta = 0.001$ (black circle), and $\mathfrak{f} = 1$, $\delta = 0.66$ for $c = 1.75$, $\theta = 0.007$ (blue triangle). These values closely align with the numerical results illustrated in the figure. The right panel displays the discrepancy between the numerical results and the predictions of Eq. (10), i.e., $|(n_{\text{numeric}} - n)/n|$, where n_{numeric} represents the mean value of the number of defects obtained numerically and n is given by Eq. (10). It demonstrates that Eq. (10) effectively predicts the number of defects generated in a phase transition with tunable order.

In this Letter, we investigated topological defect formation in a phase transition with tunable order. Such phase transitions can be observed in various systems, including superconductors, charged superfluids, and liquid crystals. It has been shown that KZM can remain effective in predicting defect density when integrated with nucleation theory.

The fraction of space $\mathfrak{f}$ occupied by the new phase due to nucleation events from the Avrami equation proves to be useful for distinguishing between regimes governed by KZM and those dominated by nucleation processes. When $\mathfrak{f} = 0$, nucleations do not occur prior to the second-order phase transition, and KZM can provide an accurate prediction of defect density. When $\mathfrak{f} = 1$, the entire space undergoes a transition to the new phase through nucleation-growth processes before the second-order phase transition, and the defect density is determined by nucleation theory. When $0 < \mathfrak{f} < 1$, we postulated that the defect density in the region covered by the new phase between times t_1 and t_2 can be described by nucleation theory, while the density in the remaining space follows KZM.

Our numerical results provide support for this conjecture. It is conceivable to validate our findings within the phase transitions of liquid crystals [45] in the future.

We thank Pablo Laguna for helpful discussions. F. S. acknowledges support from the Los Alamos National Laboratory LDRD program under Project No. 20230049DR and the Center for Nonlinear Studies under Project No. 20220546CR-NLS.

*Corresponding author: fsuzuki@lanl.gov

[1] T. W. B. Kibble, J. Phys. A **9**, 1387 (1976).
[2] T. W. B. Kibble, Phys. Rep. **67**, 183 (1980).
[3] W. H. Zurek, Nature (London) **317**, 505 (1985).
[4] W. H. Zurek, Acta Phys. Pol. B **24**, 1301 (1993).
[5] W. H. Zurek, Phys. Rep. **276**, 177 (1996).
[6] A. del Campo and W. H. Zurek, Int. J. Mod. Phys. A **29**, 1430018 (2014).
[7] A. del Campo, F. J. Gómez-Ruiz, and H.-Q. Zhang, Phys. Rev. B **106**, L140101 (2022).
[8] B. Damski, Phys. Rev. Lett. **95**, 035701 (2005).
[9] A. Polkovnikov, Phys. Rev. B **72**, 161201(R) (2005).
[10] A. Polkovnikov, K. Sengupta, A. Silva, and M. Vengalattore, Rev. Mod. Phys. **83**, 863 (2011).
[11] J. Dziarmaga, Phys. Rev. Lett. **95**, 245701 (2005).
[12] J. Dziarmaga, Adv. Phys. **59**, 1063 (2010).
[13] D. Sadhukhan, A. Sinha, A. Francuz, J. Stefaniak, M. M. Rams, J. Dziarmaga, and W. H. Zurek, Phys. Rev. B **101**, 144429 (2020).
[14] A. Francuz, J. Dziarmaga, B. Gardas, and W. H. Zurek, Phys. Rev. B **93**, 075134 (2016).
[15] J. Sonner, A. del Campo, and W. H. Zurek, Nat. Commun. **6**, 7406 (2015).
[16] W. H. Zurek, U. Dorner, and P. Zoller, Phys. Rev. Lett. **95**, 105701 (2005).
[17] L. Cincio, J. Dziarmaga, M. M. Rams, and W. H. Zurek, Phys. Rev. A **75**, 052321 (2007).
[18] F. Pollmann, S. Mukerjee, A. G. Green, and J. E. Moore, Phys. Rev. E **81**, 020101(R) (2010).
[19] A. Sinha, M. M. Rams, and J. Dziarmaga, Phys. Rev. B **99**, 094203 (2019).
[20] M. M. Rams, J. Dziarmaga, and W. H. Zurek, Phys. Rev. Lett. **123**, 130603 (2019).
[21] M. Schmitt, M. M. Rams, J. Dziarmaga, M. Heyl, and W. H. Zurek, Sci. Adv. **8**, eabl6850 (2022).
[22] R. Schützhold, M. Uhlmann, Y. Xu, and U. R. Fischer, Phys. Rev. Lett. **97**, 200601 (2006).
[23] M. Uhlmann, R. Schützhold, and U. R. Fischer, Phys. Rev. Lett. **99**, 120407 (2007).
[24] N. A. Sinitsyn, V. G. Sadhasivam, and F. Suzuki, J. Chem. Phys. **160**, 074104 (2024).
[25] F. A. Bayocboc, Jr., J. Dziarmaga, and W. H. Zurek, Phys. Rev. B **109**, 064501 (2024).
[26] M. T. Wheeler, H. Salman, and M. O. Borgh, arXiv: 2312.16555.
[27] V. G. Sadhasivam, F. Suzuki, B. Yan, and Nikolai A. Sinitsyn, arXiv:2403.09291.
[28] A. Vilenkin and E. P. S. Shellard, *Cosmic Strings and Other Topological Defects* (Cambridge University Press, Cambridge, England, 1994).
[29] *Formation and Interactions of Topological Defects*, edited by A. C. Davis and R. N. Brandenberger (Plenum, New York, 1995).
[30] A. Mazumdar and G. White, Rep. Prog. Phys. **82**, 076901 (2019).
[31] A. Maniv, E. Polturak, and G. Koren, Phys. Rev. Lett. **91**, 197001 (2003).
[32] I. Chuang, R. Durrer, N. Turok, and B. Yurke, Science **251**, 1336 (1991).
[33] M. J. Bowick, L. Chandar, E. A. Schiff, and A. M. Srivastava, Science **263**, 943 (1994).
[34] P. C. Hendry, N. S. Lawson, R. A. M. Lee, P. V. E. McClintock, and C. D. H. Williams, Nature (London) **368**, 315 (1994).
[35] V. M. H. Ruutu, V. B. Eltsov, A. J. Gill, T. W. B. Kibble, M. Krusius, Yu. G. Makhlin, B. Plaçais, G. E. Volovik, and W. Xu, Nature (London) **382**, 334 (1996).
[36] C. Bäuerle, Yu. M. Bunkov, S. N. Fisher, H. Godfrin, and G. R. Pickett, Nature (London) **382**, 332 (1996).
[37] J. Sabbatini, W. H. Zurek, and M. J. Davis, Phys. Rev. Lett. **107**, 230402 (2011).

[38] H. Saito, Y. Kawaguchi, and M. Ueda, Phys. Rev. A **76**, 043613 (2007).
[39] S. Erne, R. Buecker, T. Gasenzer, J. Berges, and J. Schmiedmayer, Nature (London) **563**, 225 (2018).
[40] B. Damski and W. H. Zurek, Phys. Rev. Lett. **104**, 160404 (2010).
[41] A. D. King *et al.*, Nat. Phys. **18**, 1324 (2022).
[42] A. Keesling *et al.*, Nature (London) **568**, 207 (2019).
[43] B. I. Halperin, T. C. Lubensky, and Shang-keng Ma, Phys. Rev. Lett. **32**, 292 (1973).
[44] A. Das, Phys. Rev. B **97**, 214429 (2018).
[45] B. Wen and C. Rosenblatt, Phys. Rev. Lett. **89**, 195505 (2002).
[46] A. Yates and W. H. Zurek, Phys. Rev. Lett. **80**, 5477 (1998).
[47] J. Dziarmaga, P. Laguna, and W. H. Zurek, Phys. Rev. Lett. **82**, 4749 (1999).
[48] N. D. Antunes, L. M. A. Bettencourt, and W. H. Zurek, Phys. Rev. Lett. **82**, 2824 (1999).
[49] P. Laguna and W. H. Zurek, Phys. Rev. Lett. **78**, 2519 (1997).
[50] M. Mielenz, J. Brox, S. Kahra, G. Leschhorn, M. Albert, T. Schaetz, H. Landa, and B. Reznik, Phys. Rev. Lett. **110**, 133004 (2013).
[51] Y. Bando, Y. Susa, H. Oshiyama, N. Shibata, M. Ohzeki, F. J. Gómez-Ruiz, D. A. Lidar, S. Suzuki, A. del Campo, and H. Nishimori, Phys. Rev. Res. **2**, 033369 (2020).
[52] K. Lee, S. Kim, T. Kim, and Y. Shin, arXiv:2310.05437.
[53] G. Schaller *et al.*, arXiv:2310.18216.
[54] M. Alford, H. Feldman, and M. Gleiser, Phys. Rev. D **47**, R2168(R) (1993).
[55] M. Alford, H. Feldman, and M. Gleiser, Phys. Rev. Lett. **68**, 1645 (1992).
[56] E. Ben-Naim and P. L. Krapivsky, Phys. Rev. E **54**, 3562 (1996).
[57] M. Sanati and A. Saxena, J. Phys. A **32**, 4311 (1999).
[58] L. Shen and G.-W. Chern, Phys. Rev. E **103**, 032134 (2021).
[59] In [1], Kibble writes "If [temperature] is only a little less than [the critical temperature] fluctuation to $\phi = 0$ will have high probability so long as the free energy required is substantially less than the thermal energy.... Thereafter fluctuations back to $\phi = 0$ rapidly become less likely, so that the distinction between normal and ordered phases is well established as is that between ordered phases corresponding to well separated points...(i.e. very different orientations...). The correlation length at this time thus determines the initial scale of the protodomains." This argument would result in the defect density independent of the quench rate.
[60] See Supplemental Material at http://link.aps.org/supplemental/10.1103/PhysRevLett.132.241601 for detailed calculations and derivations of the equations used in the main text.
[61] A. Kolmogorov, Bull. Acad. Sci. USSR Mat. Ser. **1**, 355 (1937).
[62] W. A. Johnson and R. F. Mehl, Trans. Am. Inst. Min. Metall. Eng. **135**, 416 (1939).
[63] M. Avrami, J. Chem. Phys. **7**, 1103 (1939).
[64] M. Avrami, J. Chem. Phys. **8**, 212 (1940).
[65] B. Cantor, *The Equations of Materials* (Oxford University Press, New York, 2020).
[66] S. Coleman, Phys. Rev. D **15**, 2929 (1977).
[67] A. H. Guth and S. H. H. Tye, Phys. Rev. Lett. **44**, 631 (1980).
[68] A. H. Guth and E. J. Weinberg, Phys. Rev. D **23**, 876 (1981).